derived from 4R tau isoform was detected as VQIIN*K (* indicates deamidation) (Figure 1e), while Q276 was normal, strongly suggesting that N279 is extensively deamidated in tau in AD.

RD4 cannot recognize 4R tau with deamidation at N279

Since N279 is located in the RD4 epitope, we next examined the effect of deamidation of N279 on immunoreactivity to RD4. Substitution of N279 to aspartic acid was introduced into 4R1N human tau isoform by site-directed mutagenesis, and immunoreactivity to mutant (N279D)-4R tau before and after phosphorylation by protein kinase A was compared with that of wild-type tau. As shown in Figure 2(a-d), RD4 was not able to recognize N279D-4R tau regardless of the phosphorylation state of Ser262, which is located near the RD4 epitope. To further investigate the

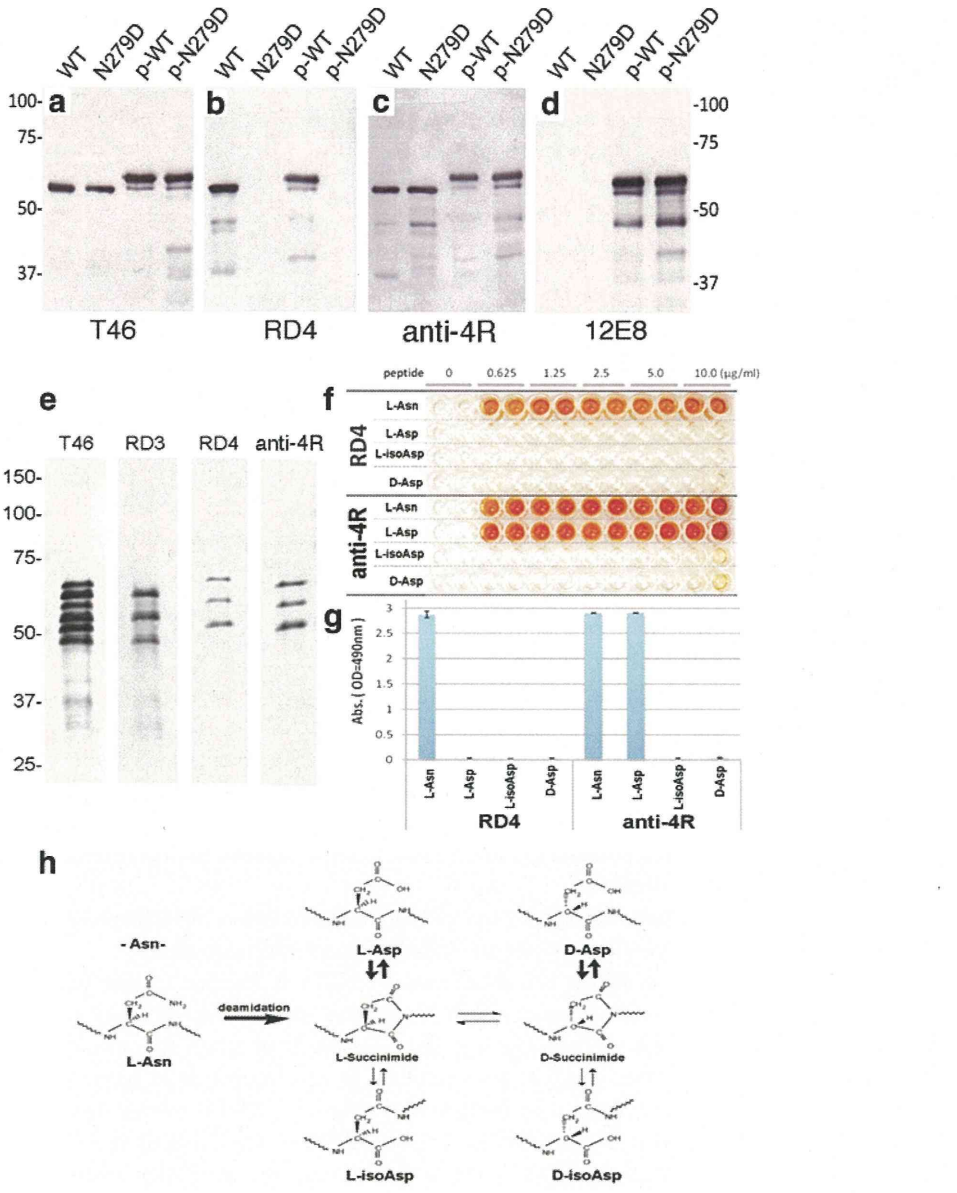

Figure 2 RD4 cannot recognize N279D-4R tau, but new anti-4R labels both WT and N279D-4R tau equally. Immunoblot analysis of wild-type (WT) and N279D mutant tau before (WT, N279D) and after (p-WT, p-N279D) phosphorylation with PKA, using T46 **(a)**, RD4 **(b)**, anti-4R **(c)** and 12E8 **(d)** antibodies. Immunoblot analysis of six recombinant human tau isoforms with T46, RD3, RD4 and anti-4R antibodies **(e)**. Specificities of RD4 (1:1000 dilutions) and anti-4R (1:3000 dilutions) antibodies for synthetic peptides, L-Asn (wild-type), L-Asp, L-isoAsp and D-Asp peptides (0.625 ~ 10 μg/mL) tested by ELISA assay **(f)**. Quantitation of the ELISA results (the mean of absorbance at 490 nm on 1.25 μg/mL peptide is shown **(g)**. Pathways for deamidation of asparaginyl residues **(h)**. L-Asn residue can be converted spontaneously via a succinimidyl intermediate to form L-Asp, D-Asp. L-isoAsp and D-isoAsp residue (modified from Ref. [9]).

deamidation of N279 of tau, we immunized a rabbit with a synthetic peptide, VQIIDKKLDLSNVQSKC, which is the RD4 antigen peptide with substitution of N279 to Asp. The antiserum anti-4R labeled both wild-type (WT) and N279D-4R tau equally (Figure 2c) and the immunoreactivity was unaffected by phosphorylation of Ser262/356 with PKA (Figure 2c). The anti-4R antibody specifically bound with recombinant human 4R tau isoforms, as did RD4, but did not react with the 3R tau isoforms (Figure 2e). The specificities of RD4 and anti-4R antibodies were further analyzed by means of ELISA assay using the antigen peptide of RD4 (L-Asn), the peptide with N279D substitution (L-Asp), the peptide with L-isoAsp substitution (L-isoAsp) and the peptide with N279 D-Asp substitution (D-Asp) (Figure 2f,g). These modifications are known to be related to deamidation of Asn residue (Figure 2h). RD4 failed to react with L-Asp (antigen peptide with N279D substitution), whereas anti-4R reacted almost equally with L-Asn (wild-type) and L-Asp peptide. Neither RD4 nor anti-4R reacted with D-Asp or L-isoAsp peptide (Figure 2f,g).

Antiserum against peptide with deamidation of N279 strongly stained tau smears in AD

The immunoreactivity of anti-4R was compared to that of RD4, RD3 and T46 in immunoblotting of Sarkosyl-insoluble tau from tauopathy brains (Figure 3). Samples of insoluble tau from three AD (lane 1–3), two PSP (lane 3, 4) and two CBD (lane 6, 7) cases were examined (Figure 3a-d). RD4 faintly stained only two bands at 64 and 68 kDa in AD brains, whereas it stained several tau fragments in PSP and CBD, in addition to the two bands at 64 and 68 (Figure 3b). In contrast, anti-4R stained tau bands and smears in AD, like RD3, and this staining was much stronger than that of tau bands and smears in PSP and CBD (Figure 3d). These results strongly suggest that tau in AD brains is predominantly deamidated at N279, and that the levels of deamidation are much lower in tau from PSP and CBD brains.

Next, we compared the immunostaining of tau pathologies with RD3, RD4 and anti-4R on formalin-fixed brain sections of AD (Figure 4). None of the three antibodies stained tau on formalin-fixed sections in the absence of formic acid treatment or autoclaving (not shown), suggesting that the epitopes of these antibodies are masked. After autoclaving or formic acid treatment, neurofibrillary tangles (NFTs) and neuropil threads (NTs) were detected with these antibodies, and dual treatment with both autoclaving and formic acid strongly enhanced the staining (not shown). The new anti-4R antibody stained intracellular NFTs and NTs more extensively than did RD4 (Figure 4). This was most evident in the CA1 region, where anti-4R strongly stained RD3+/RD4– NFTs (Figure 4d,f). This result indicates that the RD4 epitope is deamidated in pathological tau from AD brain,

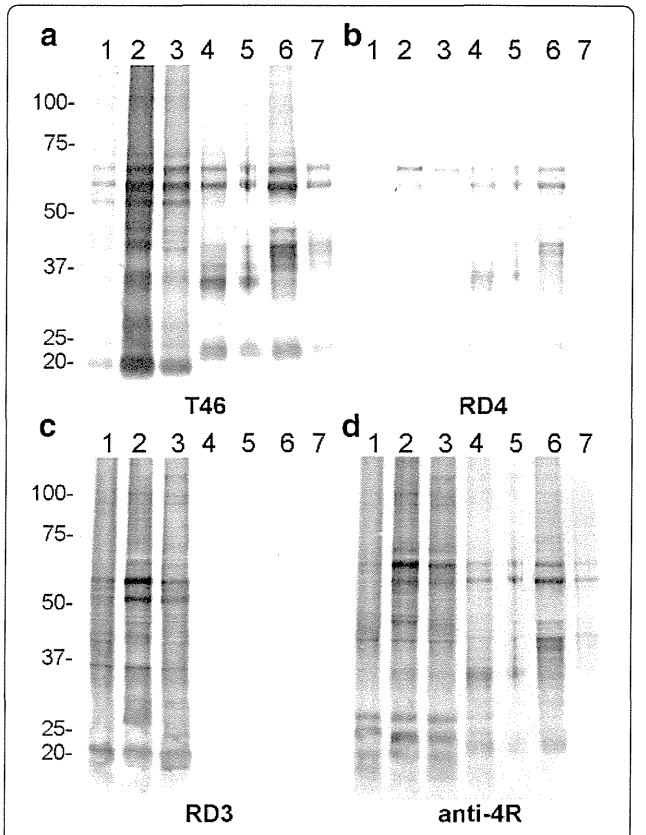

Figure 3 New anti-4R strongly stained tau bands and smears in AD. Immunoblot analyses of Sarkosyl-insoluble tau from three AD (1–3), two PSP(4, 5) and two CBD (6, 7) cases with T46 (**a**, 1:2000 dilution), RD4 (**b**, 1:1000 dilution), RD3 (**c**, 1:1000 dilution) and anti-4R antibodies (**d**, 1:2000 dilution).

especially in RD3+/RD4– NFTs. RD3 stained abundant ghost tangles in entorhinal cortex and NFTs in CA1, but failed to stain fine processes of NFTs and NTs (Figure 4), as previously reported [10]. Anti-4R also failed to detect ghost tangles in entorhinal cortex.

Deamidation of N279 reduces the ability of tau to bind microtubules

N279 is located in one of the repeat regions of tau that are involved in binding to microtubules. Therefore, we tested whether the deamidation influences the role of tau in microtubule binding and assembly. First, the ability of N279D mutant tau to mediate polymerization of tubulin was compared to that of wild-type tau by monitoring the turbidity after mixing tubulin with tau. The N279D mutant tau showed a reduced ability to promote microtubule assembly (Figure 5a). We next investigated the binding ability of the N279D mutant tau to taxol-stabilized microtubules. Tau bound and unbound to microtubules was separated by centrifugation and the levels were quantitated by means of SDS-PAGE and CBB staining (Figure 5b,c). When the amount of tau was

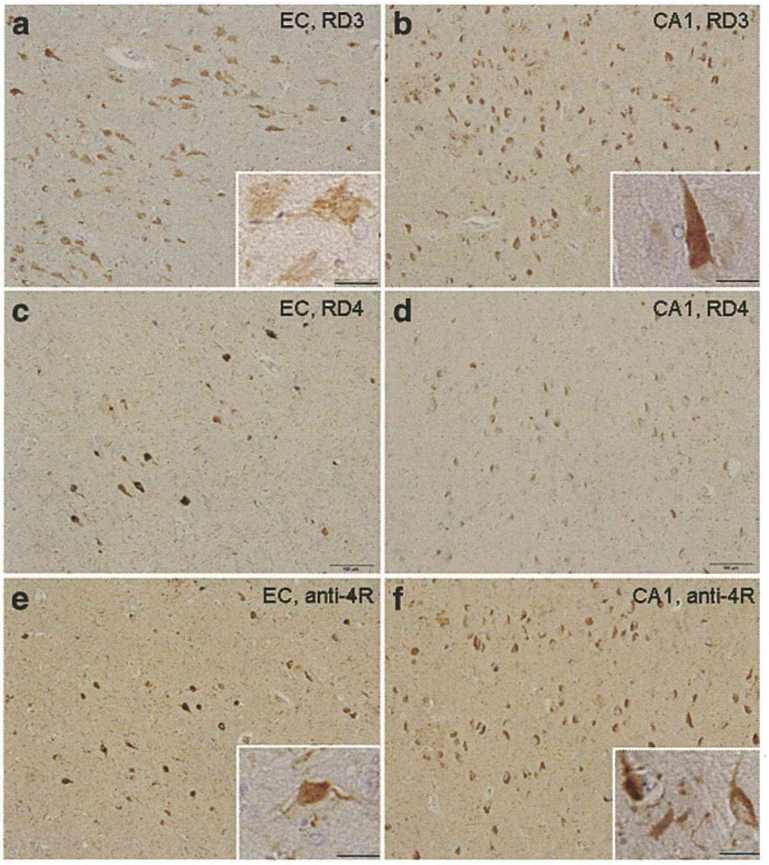

Figure 4 New anti-4R antibody stained intracellular NFTs more extensively than did RD4. Immunostaining of entorhinal cortex (EC) and CA1 sections of AD brain after autoclaving and formic acid treatments, using RD3 **(a, b)**, RD4 **(c, d)** and anti-4R **(e, f)** antibodies. NFTs with higher magnification are shown in insets. Bar = 100 μm (25 μm in insets).

increased in the presence of a constant amount of microtubules, the binding affinity and the microtubule assembly-promoting activity of N279D mutant tau were both found to be much lower than those of WT tau, clearly indicating that deamidation of N279 reduced the functional activity of tau (Figure 5b,c). Since several positively charged residues have been shown to be important for the ability of tau to promote microtubule assembly, negative charge arising from deamidation of N279 may affect the interaction.

Discussion

Our present results indicate that the N279 on the RD4 epitope is extensively deamidated in pathological tau from AD brain. Because the widely used RD4 antibody is unreactive to the deamidated epitope, the level of 4R tau isoforms in AD brain will have been markedly underestimated in previous immunohistochemical and biochemical analyses using RD4 antibody. Deamidation is an irreversible, non-enzymatic reaction, in which the amide-containing side chain is removed from asparagine or glutamine. It is known to be a marker for aging in proteins with long life-spans, and, for example, many deamidation sites have been identified in crystallins [11], the major proteins of the eye lens. In biochemical deamidation, the side chain of an asparagine residue attacks the amide group, forming a succinimide intermediate, which, upon hydrolysis, affords either aspartate or isoaspartate [12]. Isoaspartate formation from asparagine residues of tau has been reported in AD brains [9,13], but deamidation has been less well investigated. Nevertheless, deamidation is important because it alters the charge of the amino acid residue, and this can markedly affect protein structure and interaction with other proteins. Therefore, deamidation of N279 may have an effect on tau similar to that of missense mutations in FTDP-tau, many of which affect the ability of tau to promote microtubule assembly or to self-aggregate into amyloid fibrils. Indeed, substitution of N279 to Asp greatly reduced the ability of tau to promote microtubule assembly (Figure 5). However, we did not observe any accelerating effect on tau fibril formation (data not shown). Further studies are needed, but it is possible that the deamidation may be a consequence of aging of tau in paired helical filaments (PHF).

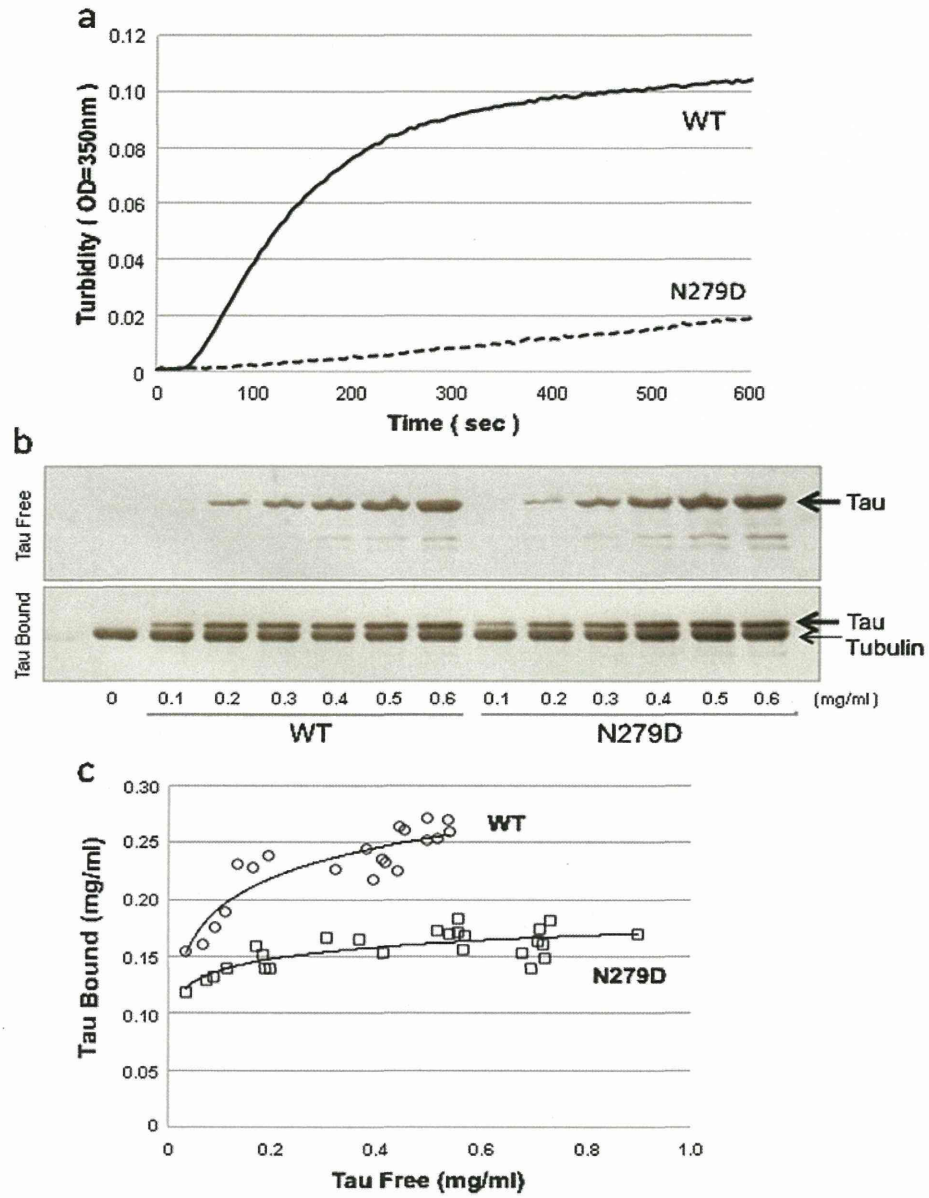

Figure 5 Deamidation of N279 reduced the functional activity of tau. Effects of deamidation at N279 on the ability of four repeat htau46 (412 amino acid isoform of human tau) to promote microtubule assembly **(a)** and to bind to microtubules **(b, c)**. **a**, Polymerisation of tubulin induced by wild-type htau46 (solid line) and htau46 N279D (dotted line) was monitored by turbidimetry. Results of a typical experiment are shown; similar results were obtained in three separate experiments. **b**, SDS-PAGE and CBB stainings of free tau and tau bound (arrows) to a constant amount of tubulin (small arrow) are shown. **c**, Scatter plots of quantitations of free tau and tau bound to WT tau (open circles) and N279D mutant tau (open squares).

Other potential post-translational modifications in the RD4 epitope include acetylation and methylation on K280 [14-16]. Using antibodies specific for tau acetylated at lysine 280, significant acetylated-tau pathology has been found with a distribution pattern similar to that of hyperphosphorylated tau [15]. However, in our protein chemical analyses (including LC/MS/MS) of AD tau, such modification has not been clearly detected. It is possible that the modification is hardly detectable in LC/MS/MS. But it is also possible that antibodies to acetylated K280 peptide may recognize a tau epitope exposed as a result of conformational change. It remains to be investigated whether the acetylation or methylation alters immunoreactivity to RD4 or whether deamidation of N279 influences immunoreactivity to acetylated K280.

The results of this study have implications for the molecular mechanisms of tau assembly. The RD4 immunoreactivity of AD tau (composed of 3R and 4R tau) is

different from that of CBD tau and PSP tau (composed of 4R tau), suggesting that the tau filament core structures may be different. Indeed, abnormal tau filaments characteristic of each disease have been described [17]. It seems reasonable to speculate that the RD4 epitope is integrated in the filament cores in CBD and PSP, making it resistant to deamidation and degradation. However, further analyses will be needed to understand the structures of tau in CBD, PSP and other tauopathies.

Prion-like spreading of intracellular pathological proteins or template (seed)-dependent conversion of normal protein to abnormal forms are candidate molecular mechanisms for involvement in the pathogenesis and progression of neurodegenerative diseases including AD [18-21]. The biochemical and structural differences of tau in AD from that in 4R tauopathies found in this study may therefore have implications for prion-like propagation of tau. Heterodimeric tau composed of both 3R tau and 4R tau with an amyloid-like conformation may act as a template for converting normal 3R and 4R tau to the abnormal structures seen in neurons, forming unique PHF structures composed of both 3R and 4R tau. Therefore, site-specific antibodies are important tools for immunohistochemical and biochemical studies of the role of tau in neurodegenerative diseases.

Conclusions

We conclude that extensive irreversible post-translational deamidation takes place at asparagine residue 279 (N279) in the RD4 epitope of tau in Alzheimer's disease (AD), but not corticobasal degeneration (CBD) or progressive supranuclear palsy (PSP), and this modification abrogates the immunoreactivity to RD4. An antiserum raised against deamidated RD4 peptide specifically recognized 4R tau isoforms, regardless of deamidation, and strongly stained tau in AD brain.

Methods

Human brain tissues

Human brain tissues were obtained from The Manchester Brain Bank, University of Manchester (Manchester, UK), Tokyo Metropolitan Institute of Gerontology (Tokyo, Japan) and NCNP Hospital (Tokyo, Japan). This study was approved by the local research ethics committees of Tokyo Institute of Psychiatry and Tokyo Metropolitan Institute of Medical Science. The subjects included three patients diagnosed with AD, three with PSP and three with CBD, neuropathologically confirmed by immunohistochemistry with antibodies to tau, Aβ, α-synuclein and TDP-43.

Preparation of sarkosyl-insoluble fractions

Brain samples (0.5 g) from patients with AD, PSP and CBD were each homogenized in 10 ml of homogenization buffer (HB: 10 mM Tris–HCl, pH 7.5 containing 0.8 M NaCl, 1 mM EGTA, 1 mM dithiothreitol). Sarkosyl was added to the lysates (final concentration: 2%), which were then incubated for 30 min at 37°C and centrifuged at 20,000 g for 10 min at 25°C. The supernatant was divided into eight tubes (each 1.3 mL) and centrifuged at 100,000 g for 20 min at 25°C. The pellets were further washed with sterile saline (0.5 mL/tube) and centrifuged at 100,000 g for 20 min. The resulting pellets were used as Sarkosyl-insoluble fraction (ppt).

LC/MS/MS analysis of sarkosyl-insoluble tau

Sarkosyl-insoluble tau from AD brains was subjected to SDS–PAGE using 4–20% polyacrylamide gel (PAGE mini, Daiichi, Tokyo). After staining with Coomassie brilliant blue R-250 (CBB), the bands corresponding to the phosphorylated tau (64 and 68 kDa) were cut out. In-gel digestion of proteins with 1 μg/ml trypsin was carried out as described previously and the resulting peptides were analyzed by an ion-trap spectrometry (Velos Pro; Thermo Fisher Scientific Inc. Waltham, MA). The MS/MS data files were searched and analyzed using the Mascot Server (Matrix Science Inc., Boston, MA).

Recombinant tau proteins

Expression constructs for six human tau isoforms in plasmid pRK172 were kindly provided by Dr. Goedert. Site-directed mutagenesis was used to change N279 to Asp (numbering refers to the 441-amino-acid isoform of human brain tau) in the four-repeat 412-amino-acid isoform (expressed from cDNA clone htau46). Wild-type and mutated tau proteins were expressed in *Escherichia coli* BL21(DE3) and purified as described previously[22]. For *in vitro* phosphorylation, purified tau (10 μg/ml) was incubated with PKA (10,000 U/ml; New England Biolabs, Beverly, MA) in 30 mM Tris–HCl buffer (pH 7.5) containing 0.1 mM EGTA, 10 mM $MgSO_4$, 0.8 mM PMSF and 2 mM ATP, at 30°C for 1 hr.

Antibodies

RD3 (directed to residues 209~224: Millipore), RD4 (residues 275~291: Millipore), T46 (residues 404~441: Invitrogen) and pS396 (phospho-Ser396: Calbiochem) were purchased. Antiserum anti-4R was raised against a synthetic peptide VQIIDKKLDLSNVQSKC which corresponds to residues 275~291 of human tau (441 residues), with substitution of N279 to Asp (Sigma Aldrich Japan). The peptide was conjugated to m-maleimidobenzoyl- N-hydrosuccinimide ester-activated keyhole limpet hemocyanin (KLH). The KLH-peptide complex (1 mg of each immunogen) emulsified in Freund's complete adjuvant was injected subcutaneously into a New Zealand White rabbit, followed by 5 weekly subcutaneous injections of 150 μg KLH-peptide complex emulsified in Freund's

incomplete adjuvant, starting 3 weeks after the first immunization.

ELISA assay

Each synthetic peptide consisting of residues 275~291 (VQIINKKLDLSNVQSKC) with the fifth position being replaced by L-Asp, L-isoAsp, or D-Asp was synthesized by the solid-phase method (Sigma Aldrich Japan) These peptides, L-Asn (wild-type), L-Asp, L-isoAsp, D-Asp (0.625 ~ 10 μg/ml in 50 mM Tris–HCl, pH 8.8) were coated onto microtitre plates (SUMILON) at 4°C for 16 h. The plates were blocked with 10% fetal bovine serum (FBS) in PBS, incubated with the first antibodies (RD4, 1:1000; anti-4R, 1:3000) diluted in 10% FBS/PBS at room temperature for 1.5 h, followed by incubation with HRP-goat anti-rabbit IgG (Bio-Rad) at 1:1000 dilution, and reacted with the substrate, 0.4 mg/ml o-phenylendiamine, in citrate buffer (24 mM citric acid, 51 mM Na_2HPO_4), The absorbance at 490 nm was measured using Plate Chameleon (HIDEX) as described [23].

Microtubule assembly and tau binding

Purified recombinant wild-type and mutant tau (htau46) proteins (0.1 mg/ml, 2.3 μM) were incubated with bovine brain tubulin (1 mg/ml, 20 μM, cytoskeleton) in assembly buffer at 37°C, as described [22]. The assembly of tubulin was monitored in terms of the change in turbidity at 350 nm. The binding assay was performed as described [24]. Briefly, purified tubulin was incubated at 37°C in the presence of 1 mM GTP and 20 μM taxol. Tau protein was added at various concentrations and each mixture was incubated for 10 min. The suspensions were centrifuged for 100,000 g at 37°C. The resulting pellets were resuspended in 50 mM PIPES pH 6.9, 1 mM EGTA, 0.2 mM $MgCl_2$, 5 mM DTT, 0.5 M NaCl. The pellets and supernatants (containing bound and free tau, respectively) were subjected to SDS-PAGE and stained with Coomassie brilliant blue R250. The gels were scanned at 400 dpi on a gel scanner and evaluated using the software provided.

Gel electrophoresis and immunoblotting

Samples were run on gradient 4-20% or 10% polyacrylamide gels and electrophoretically transferred to PVDF membranes. Residual protein-binding sites were blocked by incubation with 3% gelatin (Wako) for 10 min at 37°C, followed by overnight incubation at room temperature with the primary antibody. The membrane was then incubated for 1 hr at room temperature with anti-rabbit IgG (BA-1000, Vector Lab) or anti-mouse IgG (BA-2000, Vector lab), then incubated for 30 min with avidin-horseradish peroxidase (Vector Lab), and the reaction product was visualized by using 0.1% 3,3-diaminobenzidine (DAB) and 0.2 mg/ml $NiCl_2$ as the chromogen.

Immunohistochemistry

Formalin-fixed paraffin-embedded sections of AD brains were used for immunohistochemistry. The sections were pretreated by autoclaving for 10 min in 10 mM sodium citrate buffer at 120°C and treated with 100% formic acid for 10 min. Sections were washed with 10 mM phosphate-buffered saline (PBS, pH 7.4) three times for 10 min each. Sections were blocked with 10% normal serum and incubated overnight at room temperature with one of the primary antibodies in PBS. After washing, sections were incubated with biotinylated anti-mouse or rabbit secondary antibody for 2 h, followed by biotinylated horseradish peroxidase complex (ABC, Vector) for 1 hr. The label was visualized with EnVision™(Dako). Sections were counterstained with hematoxylin.

Competing interests

The authors declare that they have no competing interests.

Authors' contributions

AD, MT, MS and TN performed biochemical and immunochemical studies. FK performed LC/MS/MS analysis. HK performed immunohistochemistry. TA helped for characterisation of antibody. HA, YS, HH, SM and DM performed neuropathological studies and analyses. MH performed study design, preparation of antibody, biochemical analyses and wrote the paper. All authors read and approved the final manuscript.

Acknowledgements

We acknowledge the support of Alzheimer's Research UK and Alzheimer's Society through their funding of the Manchester Brain Bank under the Brains for Dementia Research (BDR) initiative. This work was supported by a Grant-in-Aid for Scientific Research (S) (JSPS KAKENHI 23228004 to M.H.), a Grant-in-Aid for Scientific Research (A) (JSPS KAKENHI 23240050 to M.H.), MHLW Grant (Number 12946221 to M.H.) and a Grant-in-Aid for Scientific Research on Innovative Area 'Brain Environment' (MEXT KAKENHI 24111556 to T.N).

Author details

[1]Department of Neuropathology and Cell Biology, Tokyo Metropolitan Institute of Medical Science, Setagaya-ku, Tokyo 156-8506, Japan. [2]Histology center, Tokyo Metropolitan Institute of Medical Science, Setagaya-ku, Tokyo 156-8506, Japan. [3]Dementia Research Project, Tokyo Metropolitan Institute of Medical Science, Setagaya-ku, Tokyo 156-8506, Japan. [4]Department of Applied Biological Science, Faculty of Science and Technology, Tokyo University of Science, 2641 Yamazaki, Noda-shi, Chiba-ken 278-8510, Japan. [5]Centre for Clinical and Cognitive Neuroscience, Institute of Brain Behavior and Mental Health, University of Manchester, Salford M6 8HD, UK. [6]Department of Laboratory Medicine, National Center Hospital, NCNP, 4-1-1 Ogawahigashi, Kodaira, Tokyo 187-8502, Japan. [7]Department of Neuropathology, Tokyo Metropolitan Institute of Gerontology, Itabashi-ku, Tokyo 173-0015, Japan.

Received: 17 August 2013 Accepted: 17 August 2013
Published: 21 August 2013

References

1. Umeda Y, Taniguchi S, Arima K, Piao YS, Takahashi H, Iwatsubo T, Mann D, Hasegawa M: **Alterations in human tau transcripts correlate with those of neurofilament in sporadic tauopathies.** *Neurosci Lett* 2004, **359**:151–154.
2. Goedert M, Spillantini MG: **Pathogenesis of the tauopathies.** *J Mol Neurosci* 2011, **45**:425–431.
3. Arai T, Ikeda K, Akiyama H, Nonaka T, Hasegawa M, Ishiguro K, Iritani S, Tsuchiya K, Iseki E, Yagishita S, Oda T, Mochizuki A: **Identification of amino-terminally**

cleaved tau fragments that distinguish progressive supranuclear palsy from corticobasal degeneration. *Ann Neurol* 2004, **55**:72–79.

4. de Silva R, Lashley T, Gibb G, Hanger D, Hope A, Reid A, Bandopadhyay R, Utton M, Strand C, Jowett T, Khan N, Anderton B, Wood N, Holton J, Revesz T, Lees A: **Pathological inclusion bodies in tauopathies contain distinct complements of tau with three or four microtubule-binding repeat domains as demonstrated by new specific monoclonal antibodies.** *Neuropathol Appl Neurobiol* 2003, **29**:288–302.
5. de Silva R, Lashley T, Strand C, Shiarli AM, Shi J, Tian J, Bailey KL, Davies P, Bigio EH, Arima K, Iseki E, Murayama S, Kretzschmar H, Neumann M, Lippa C, Halliday G, MacKenzie J, Ravid R, Dickson D, Wszolek Z, Iwatsubo T, Pickering-Brown SM, Holton J, Lees A, Revesz T, Mann DM: **An immunohistochemical study of cases of sporadic and inherited frontotemporal lobar degeneration using 3R- and 4R-specific tau monoclonal antibodies.** *Acta Neuropathol* 2006, **111**:329–340.
6. Togo T, Akiyama H, Iseki E, Uchikado H, Kondo H, Ikeda K, Tsuchiya K, de Silva R, Lees A, Kosaka K: **Immunohistochemical study of tau accumulation in early stages of Alzheimer-type neurofibrillary lesions.** *Acta Neuropathol* 2004, **107**:504–508.
7. Piao YS, Tan CF, Iwanaga K, Kakita A, Takano H, Nishizawa M, Lashley T, Revesz T, Lees A, de Silva R, Tsujihata M, Takahashi H: **Sporadic four-repeat tauopathy with frontotemporal degeneration, parkinsonism and motor neuron disease.** *Acta Neuropathol* 2005, **110**:600–609.
8. Hasegawa M, Morishima-Kawashima M, Takio K, Suzuki M, Titani K, Ihara Y: **Protein sequence and mass spectrometric analyses of tau in the Alzheimer's disease brain.** *J Biol Chem* 1992, **267**:17047–17054.
9. Watanabe A, Takio K, Ihara Y: **Deamidation and isoaspartate formation in smeared tau in paired helical filaments. Unusual properties of the microtubule-binding domain of tau.** *J Biol Chem* 1999, **274**:7368–7378.
10. Hara M, Hirokawa K, Kamei S, Uchihara T: **Isoform transition from four-repeat to three-repeat tau underlies dendrosomatic and regional progression of neurofibrillary pathology.** *Acta Neuropathol* 2013, **125**:565–579.
11. Van Kleef FS, De Jong WW, Hoenders HJ: **Stepwise degradations and deamidation of the eye lens protein alpha-crystallin in ageing.** *Nature* 1975, **258**:264–266.
12. Geiger T, Clarke S: **Deamidation, isomerization, and racemization at asparaginyl and aspartyl residues in peptides. Succinimide-linked reactions that contribute to protein degradation.** *J Biol Chem* 1987, **262**:785–794.
13. Miyasaka T, Watanabe A, Saito Y, Murayama S, Mann DM, Yamazaki M, Ravid R, Morishima-Kawashima M, Nagashima K, Ihara Y: **Visualization of newly deposited tau in neurofibrillary tangles and neuropil threads.** *J Neuropathol Exp Neurol* 2005, **64**:665–674.
14. Cohen TJ, Guo JL, Hurtado DE, Kwong LK, Mills IP, Trojanowski JQ, Lee VM: **The acetylation of tau inhibits its function and promotes pathological tau aggregation.** *Nat Commun* 2011, **2**:252.
15. Irwin DJ, Cohen TJ, Grossman M, Arnold SE, Xie SX, Lee VM, Trojanowski JQ: **Acetylated tau, a novel pathological signature in Alzheimer's disease and other tauopathies.** *Brain* 2012, **135**:807–818.
16. Min SW, Cho SH, Zhou Y, Schroeder S, Haroutunian V, Seeley WW, Huang EJ, Shen Y, Masliah E, Mukherjee C, Meyers D, Cole PA, Ott M, Gan L: **Acetylation of tau inhibits its degradation and contributes to tauopathy.** *Neuron* 2010, **67**:953–966.
17. Arima K: **Ultrastructural characteristics of tau filaments in tauopathies: immuno-electron microscopic demonstration of tau filaments in tauopathies.** *Neuropathology* 2006, **26**:475–483.
18. Clavaguera F, Akatsu H, Fraser G, Crowther RA, Frank S, Hench J, Probst A, Winkler DT, Reichwald J, Staufenbiel M, Ghetti B, Goedert M, Tolnay M: **Brain homogenates from human tauopathies induce tau inclusions in mouse brain.** *Proc Natl Acad Sci U S A* 2013, **110**:9535–9540.
19. Masuda-Suzukake M, Nonaka T, Hosokawa M, Oikawa T, Arai T, Akiyama H, Mann DM, Hasegawa M: **Prion-like spreading of pathological alpha-synuclein in brain.** *Brain* 2013, **136**:1128–1138.
20. Hasegawa M, Nonaka T, Tsuji H, Tamaoka A, Yamashita M, Kametani F, Yoshida M, Arai T, Akiyama H: **Molecular dissection of TDP-43 proteinopathies.** *J Mol Neurosci* 2011, **45**:480–485.
21. Nonaka T, Masuda-Suzukake M, Arai T, Hasegawa Y, Akatsu H, Obi T, Yoshida M, Murayama S, Mann DM, Akiyama H, Hasegawa M: **Prion-like Properties of Pathological TDP-43 Aggregates from Diseased Brains.** *Cell Rep* 2013, **4**:124–134.
22. Hasegawa M, Smith MJ, Goedert M: **Tau proteins with FTDP-17 mutations have a reduced ability to promote microtubule assembly.** *FEBS Lett* 1998, **437**:207–210.
23. Masuda M, Hasegawa M, Nonaka T, Oikawa T, Yonetani M, Yamaguchi Y, Kato K, Hisanaga S, Goedert M: **Inhibition of alpha-synuclein fibril assembly by small molecules: analysis using epitope-specific antibodies.** *FEBS Lett* 2009, **583**:787–791.
24. Gustke N, Steiner B, Mandelkow EM, Biernat J, Meyer HE, Goedert M, Mandelkow E: **The Alzheimer-like phosphorylation of tau protein reduces microtubule binding and involves Ser-Pro and Thr-Pro motifs.** *FEBS Lett* 1992, **307**:199–205.

doi:10.1186/2051-5960-1-54
Cite this article as: Dan *et al.*: Extensive deamidation at asparagine residue 279 accounts for weak immunoreactivity of tau with RD4 antibody in Alzheimer's disease brain. *Acta Neuropathologica Communications* 2013 **1**:54.

Cell PRESS
Open ACCESS

Cell Reports
Article

Prion-like Properties of Pathological TDP-43 Aggregates from Diseased Brains

Takashi Nonaka,[1,*] Masami Masuda-Suzukake,[1] Tetsuaki Arai,[2,3] Yoko Hasegawa,[1] Hiroyasu Akatsu,[4] Tomokazu Obi,[5] Mari Yoshida,[6] Shigeo Murayama,[7] David M.A. Mann,[8] Haruhiko Akiyama,[2] and Masato Hasegawa[1,*]
[1]Department of Neuropathology and Cell Biology
[2]Dementia Research Project
Tokyo Metropolitan Institute of Medical Science, Setagaya-ku, Tokyo 156-8506, Japan
[3]Division of Clinical Medicine, Department of Neuropsychiatry, Faculty of Medicine, University of Tsukuba, Tsukuba, Ibaraki 305-8575, Japan
[4]Choju Medical Institute, Fukushimura Hospital, Toyohashi, Aichi 441-8124, Japan
[5]Shizuoka Institute of Epilepsy and Neurological Disorders, Shizuoka, Shizuoka 420-8688, Japan
[6]Institute for Medical Science of Aging, Aichi Medical University, Nagakute, Aichi 480-1195, Japan
[7]Department of Neuropathology, Tokyo Metropolitan Institute of Gerontology, Itabashi-ku, Tokyo 173-0015, Japan
[8]Centre for Clinical and Cognitive Neuroscience, Institute of Brain Behavior and Mental Health, University of Manchester, Salford M6 8HD, UK
*Correspondence: nonaka-tk@igakuken.or.jp (T.N.), hasegawa-ms@igakuken.or.jp (M.H.)
http://dx.doi.org/10.1016/j.celrep.2013.06.007

SUMMARY

TDP-43 is the major component protein of ubiquitin-positive inclusions in brains of patients with frontotemporal lobar degeneration (FTLD-TDP) or amyotrophic lateral sclerosis (ALS). Here, we report the characterization of prion-like properties of aggregated TDP-43 prepared from diseased brains. When insoluble TDP-43 from ALS or FTLD-TDP brains was introduced as seeds into SH-SY5Y cells expressing TDP-43, phosphorylated and ubiquitinated TDP-43 was aggregated in a self-templating manner. Immunoblot analyses revealed that the C-terminal fragments of insoluble TDP-43 characteristic of each disease type acted as seeds, inducing seed-dependent aggregation of TDP-43 in these cells. The seeding ability of insoluble TDP-43 was unaffected by proteinase treatment but was abrogated by formic acid. One subtype of TDP-43 aggregate was resistant to boiling treatment. The insoluble fraction from cells harboring TDP-43 aggregates could also trigger intracellular TDP-43 aggregation. These results indicate that insoluble TDP-43 has prion-like properties that may play a role in the progression of TDP-43 proteinopathy.

INTRODUCTION

Frontotemporal lobar degeneration (FTLD) and amyotrophic lateral sclerosis (ALS) are well-known neurodegenerative disorders. FTLD is the second most common form of cortical dementia in the population below the age of 65 years (Snowden et al., 2002). ALS is the most common form of motor neuron disease and is characterized by progressive weakness and muscular wasting, and death within a few years. Ubiquitin-positive inclusions composed of misfolded proteins in neuronal and glial cells are common neuropathological features of most neurodegenerative diseases, including Alzheimer's disease (AD), Parkinson's disease (PD), FTLD, and ALS. Recently, TAR DNA-binding protein of 43 kDa (TDP-43) was identified as the major component of inclusions found in the brains of patients with ALS and FTLD (FTLD-U or FTLD-TDP) (Arai et al., 2006; Neumann et al., 2006). TDP-43, a 414-amino-acid protein expressed in nuclei, belongs to the heterogeneous ribonucleoprotein family, members of which are involved in repression of gene transcription, regulation of exon splicing, and nuclear body functions (Buratti and Baralle, 2009; Buratti et al., 2001). TDP-43 is thought to be essential for early embryonic development, because homozygous disruption of the TDP-43 gene (*TARDBP*) causes early embryonic lethality (Sephton et al., 2010; Wu et al., 2010). Interestingly, affected neurons containing cytoplasmic TDP-43 inclusions show depletion of normal nuclear TDP-43 (Arai et al., 2006; Neumann et al., 2006). Patients with these diseases show autosomal-dominant missense mutations in the *TARDBP* gene, mostly located in the C-terminal glycine-rich region (Pesiridis et al., 2009), and pathological TDP-43 is hyperphosphorylated, ubiquitinated, and abnormally cleaved to generate aggregation-prone C-terminal fragments (CTFs) (Arai et al., 2010; Hasegawa et al., 2008, 2011). Thus, loss of normal function of nuclear TDP-43 due to cytoplasmic mislocalization, and toxic gain of function due to cytoplasmic TDP-43 aggregation are potential disease mechanisms (Arai et al., 2006; Neumann et al., 2006).

Aberrant protein aggregates in affected neurons are well-known hallmarks of neurodegenerative diseases, but the mechanisms involved remain unclear. Recent reports suggest that prion-like propagation of protein aggregates composed of tau- or α-synuclein may be involved in progression of neurodegenerative diseases such as AD or PD. This is consistent with findings that tau- or α-synuclein pathology spreads in a

stereotypical temporal and topological manner (Braak and Braak, 1991; Braak et al., 2003). Furthermore, fetal mesencephalic grafts in the striatum of PD patients eventually develop Lewy bodies, suggesting that pathologic α-synuclein could be transmitted from diseased striatal neurons to grafted neurons (Kordower et al., 2008; Li et al., 2008). Cell-cell transmission of tau- and α-synuclein aggregates has been observed in both cell culture and animal models (Clavaguera et al., 2009; de Calignon et al., 2012; Desplats et al., 2009; Frost et al., 2009; Goedert et al., 2010; Liu et al., 2012; Luk et al., 2009, 2012a, 2012b; Nonaka et al., 2010; Masuda-Suzukake et al., 2013). Therefore, prion-like propagation of aberrant protein aggregates may be involved in the pathogenesis of neurodegenerative diseases.

Here, we show that insoluble TDP-43 aggregates in brains of ALS and FTLD-TDP patients have prion-like properties, including the ability to seed intracellular TDP-43 aggregation, stability against heat and proteinases, and cell-to-cell transmissibility.

RESULTS

Intracellular TDP-43 Is Aggregated in a Seed-Dependent Manner

The C-terminal portion of TDP-43 has sequence similarity to prion (Guo et al., 2011). Therefore, to investigate whether intracellular TDP-43 is aggregated in a self-templating manner, like prion, we first established a cell culture model for seeded aggregation of intracellular TDP-43 using SH-SY5Y and 293T cells (Figures 1 and S1A).

We examined whether TDP-43 forms intracellular aggregates in the presence of insoluble TDP-43 prepared from ALS or FTLD-TDP brains as seeds. We observed filamentous structures that were positive for antiphospho TDP-43 (anti-pS409/410) antibody (10–15 nm in diameter) by electron microscopy analyses of insoluble TDP-43 from brains of patients (Figure 1A). Furthermore, it was recently reported that TDP-43 inclusions in ALS and FTLD-TDP showed thioflavin positivity (Bigio et al., 2013). These results clearly indicate that insoluble TDP-43 from brains, used as seeds, had the properties of amyloid. To distinguish plasmid-derived TDP-43 from insoluble TDP-43 introduced as seeds, we used a plasmid encoding hemagglutinin (HA)-tagged TDP-43. SH-SY5Y cells were transiently transfected with HA-tagged TDP-43 and then transduced with or without N-lauroylsarcosine sodium salt (sarkosyl)-insoluble fraction (Sar-ppt) prepared from the brains of ALS (ALS ppt) or FTLD-TDP (FTLD ppt) patients. Cell lysates were fractionated and immunoblotted with anti-HA and anti-pS409/410 antibodies. In cells transfected with HA-TDP-43 plasmid alone, expressed HA-TDP-43 was detected in all fractions with an antibody against HA, whereas phosphorylated HA-TDP-43 was modestly detected in the insoluble fraction (ppt), indicating that the transiently expressed HA-TDP-43 was slightly aggregated (Figure 1B). In cells treated with ALS ppt (5 μg) alone, several bands were detected in ppt fractions with anti-pS409/410, suggesting that endogenous TDP-43 is aggregated in the presence of seeds. On the other hand, in HA-TDP-43-expressing cells transduced with ALS ppt (5 μg), bands with slower mobility were seen with an antibody against HA, and both phosphorylated full-length HA-TDP-43 and its CTFs were detected with anti-pS409/410. We confirmed that plasmid-derived TDP-43, but not ALS ppt seeds, is mainly aggregated in ppt fractions, because no bands were detected with anti-pS409/410 when ALS ppt (5 μg, used as seeds) alone was loaded on the gel (Figure 1C, rightmost lane). Similarly, full-length HA-TDP-43 and CTFs positive for anti-pS409/410 were produced in cells transfected with both HA-TDP-43 plasmid and FTLD ppt (Figures 1B and S1B). Given that plasmid-derived, nontagged TDP-43 was accumulated intracellularly in the presence of ALS ppt (Figure 1C), we mainly used a plasmid encoding, nontagged TDP-43 in subsequent work.

To test whether insoluble TDP-43 in diseased brain extracts can function as seeds for aggregation, we prepared immunodepleted ALS ppt (Figure 1D) as seeds for intracellular TDP-43 aggregation. Sar-ppt of ALS brain was incubated with a mixture of anti-TDP-43 (polyclonal; Proteintech) and anti-pS409/410 antibodies, followed by addition of protein G-Sepharose. After overnight incubation, the supernatant fraction was analyzed by immunoblotting. As shown in Figure 1D (left panel), the immunoreactivity against anti-pS409/410 found in nontreated ALS ppt was wholly lost after immunodepletion (ID). Then, we introduced immunodepleted ALS ppt (ALS ppt ID) into cells expressing HA-TDP-43, using MultiFectam. As shown in Figure 1D (right panel), the band intensities of phosphorylated full-length HA-TDP-43 and CTFs in the ppt fraction of cells expressing HA-TDP-43 and treated with ALS ppt ID were much weaker than those in the case of cells expressing HA-TDP-43 and treated with nonimmunodepleted ALS ppt. We also tested the specificity of ALS ppt as seeds for aggregation of TDP-43. When recombinant α-synuclein fibrils were introduced into cells transiently expressing α-synuclein, phosphorylated α-synuclein was accumulated in Triton-insoluble fractions (Figure S2A), as previously reported (Nonaka et al., 2010). However, intracellular α-synuclein aggregation was not observed in cells expressing α-synuclein and treated with ALS ppt (Figure S2B). Furthermore, HA-TDP-43 was not aggregated in the presence of α-synuclein fibril seeds (Figure S2C). These results showed that insoluble TDP-43 functions specifically as seeds for intracellular aggregation of TDP-43, but not for aggregation of α-synuclein.

We performed immunocytochemical analyses of cells expressing HA-TDP-43 and treated with or without ALS ppt. No phosphorylated and aggregated TDP-43 was seen in cells expressing HA-TDP-43 only (Figure 1E). A few dot-like structures positive for anti-pS409/410 were found in nontransfected cells treated with ALS ppt. On the other hand, round cytoplasmic inclusions of TDP-43 positive for both anti-pS409/410 and an antibody against Ub were detected in cells expressing HA-TDP-43 and treated with ALS ppt. The percentage of HA-positive cells that were also positive for anti-pS409/410 antibody was calculated to be 11.4% ± 4.3%. Interestingly, the immunoreactivity of an antibody against HA in nuclei of cells with cytoplasmic TDP-43 aggregates was less than that in nuclei of cells expressing HA-TDP-43 without aggregates (Figure 1E, lower left), as seen for pathogenic neurons with cytoplasmic TDP-43 inclusions in ALS and FTLD-TDP brains. Taken together, these results suggest that intracellular TDP-43 was efficiently aggregated in cultured cells in a manner that depended on seeding with insoluble TDP-43 derived from patients' brains.

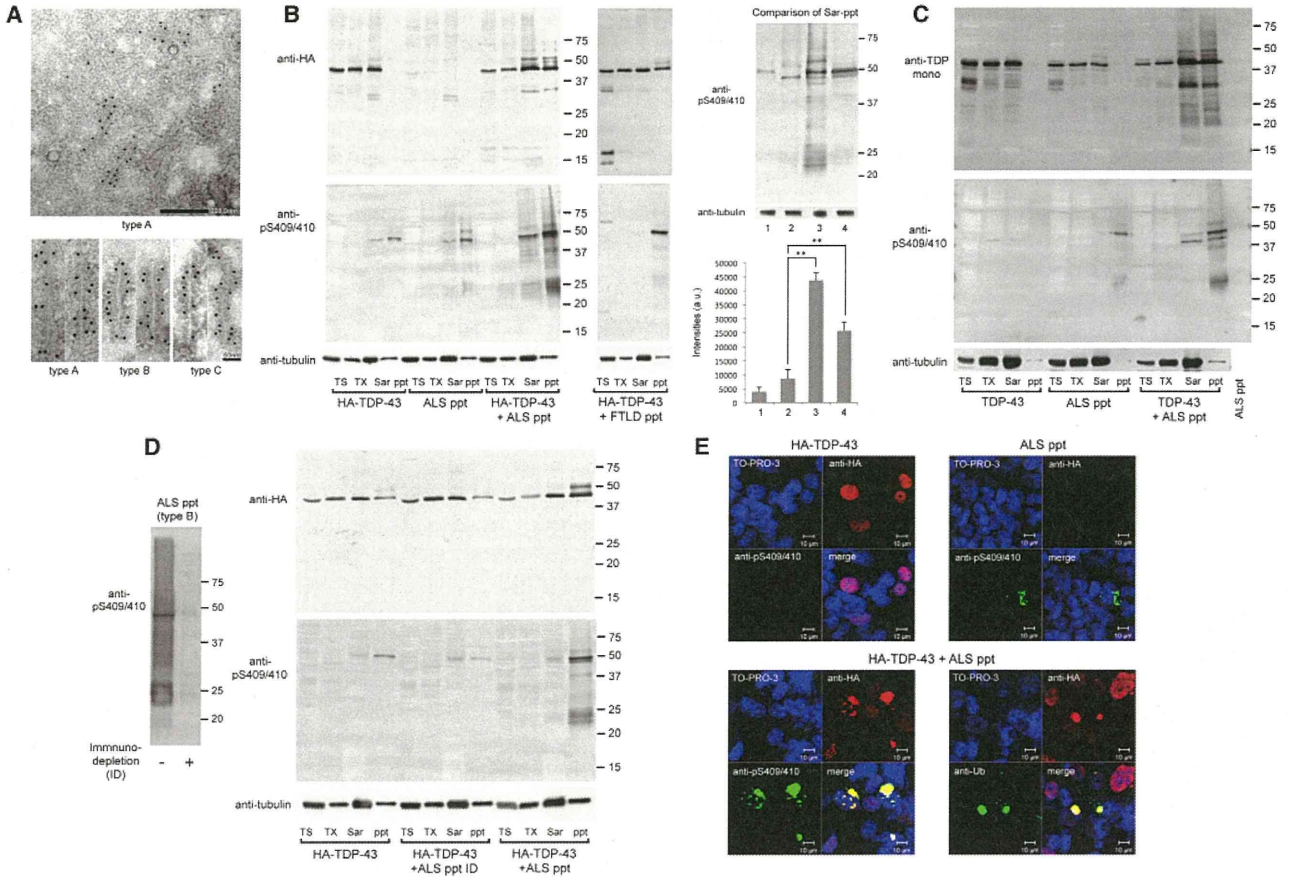

Figure 1. Detergent-Insoluble Fractions from ALS and FTLD-TDP Brains Function as Seeds for Intracellular Aggregation of Plasmid-Derived TDP-43

(A) Immuno-electron microscopy analyses of insoluble fractions from diseased brains (types A, B, and C). Filamentous structures are labeled with anti-phospho TDP-43 antibody (pS409/410). Scale bars represent 200 nm in upper panel, 50 nm in lower panel.

(B) Immunoblot analysis of lysates from cells expressing HA-TDP-43 plasmid only (HA-TDP-43), cells treated with ALS ppt (5 μg; ALS ppt), cells transfected with both HA-TDP-43 and ALS ppt (HA-TDP-43 + ALS ppt), and cells transfected with both HA-TDP-43 and FTLD ppt (5 μg; HA-TDP-43 + FTLD ppt). Proteins were differentially extracted from cells with Tris-HCl (TS), Triton X-100 (TX), and sarkosyl (Sar), leaving the pellet (ppt). Blots were probed using anti-HA (upper) and anti-pS409/410 (lower). In the right panel, the Sar-ppt fractions are shown side by side. 1: HA-TDP-43; 2: ALS ppt; 3: HA-TDP-43 + ALS ppt; 4: HA-TDP-43 + FTLD ppt. The immunoreactivity of each lane that was positive for anti-pS409/410 was quantified and the results are expressed as means + SEM (n = 3). $^{**}p < 0.0005$ by Student's t test; a.u., arbitrary unit.

See also Figure S1.

(C) Immunoblot analysis of proteins extracted from cells expressing only nontagged TDP-43 plasmid (TDP-43), cells treated only with ALS ppt (ALS ppt), and cells transfected with both TDP-43 and ALS ppt (TDP-43 + ALS ppt). Blots were probed using anti-TDP-43 monoclonal antibody (upper) and anti-pS409/410 (lower). No bands were detected when only ALS ppt (5 μg) used as seeds was loaded on the gel (rightmost lane).

(D) ID of ALS ppt was performed with (+) or without (–) a mixture of anti-TDP-43 and anti-pS409/410 antibody. This was followed by immunoblot analyses with anti-pS409/410 (left panel). Proteins differentially extracted from cells expressing only HA-TDP-43 plasmid (HA-TDP-43), and cells transfected with both HA-TDP-43 and immunodepleted ALS ppt (HA-TDP-43 + ALS ppt ID) or untreated ALS ppt (HA-TDP-43 + ALS ppt) were analyzed. Blots were probed using anti-HA (upper) and anti-pS409/410 (lower).

(E) Confocal laser microscopy analyses of cells expressing only HA-TDP-43 plasmid (HA-TDP-43), cells treated with detergent-insoluble fraction of ALS brain (ALS ppt), and cells transfected with both HA-TDP-43 and ALS ppt (HA-TDP-43 + ALS ppt) immunostained with anti-HA (red), anti-pS409/410 (green) or anti-Ub (green), and counterstained with TO-PRO-3 (blue). Scale bars represent 10 μm.

Aggregation of Full-Length TDP-43 Precedes Generation of TDP-43 CTFs

To further investigate the seed-dependent intracellular aggregation of TDP-43, we performed time-course experiments and immunoblot analyses during TDP-43 aggregate formation. Cells expressing HA-TDP-43 and treated with or without ALS ppt were incubated for 1–3 days, and each day the cell lysates were fractionated as described above. No band positive for anti-pS409/410 was detected in any fraction on day 1 or day 2, whereas a weak band of phosphorylated HA-TDP-43 was seen in the insoluble fraction (ppt) on day 3 of cells expressing HA-TDP-43 (Figure 2A). When cells were transfected with both HA-TDP-43